Astronomy
&
Astrophysics

Radio/X-ray correlation in the low/hard state of GX 339–4

S. Corbel[1], M. A. Nowak[2], R. P. Fender[3], A. K. Tzioumis[4], and S. Markoff[5]

[1] Université Paris VII and Service d'Astrophysique (Fédération APC), CEA Saclay, 91191 Gif-sur-Yvette, France

[2] Chandra X-ray Science Center, Massachusetts Institute of Technology, NE80-6077, 77 Massachusetts Ave., Cambridge MA 02139, USA

[3] Astronomical Institute "Anton Pannekoek", University of Amsterdam and Center for High Energy Astrophysics, Kruislaan 403, 1098 SJ Amsterdam, The Netherlands

[4] Australia Telescope National Facility, CSIRO, PO Box 76, Epping NSW 1710, Australia

[5] Massachusetts Institute of Technology, Center for Space Research, NE80-6035, 77 Massachusetts Ave., Cambridge MA 02139, USA

Abstract. We present the results of a long-term study of the black hole candidate GX 339−4 using simultaneous radio (from the Australia Telescope Compact Array) and X-ray (from the Rossi X-ray Timing Explorer and BeppoSAX) observations performed between 1997 and 2000. We find strong evidence for a correlation between these two emission regimes that extends over more than three decades in X-ray flux, down to the quiescence level of GX 339−4. This is the strongest evidence to date for such strong coupling between radio and X-ray emission. We discuss these results in light of a jet model that can explain the radio/X-ray correlation. This could indicate that a significant fraction of the X-ray flux that is observed in the low-hard state of black hole candidates may be due to optically thin synchrotron emission from the compact jet.

Key words. black hole physics – radiation mechanisms: non-thermal – ISM: jets and outflows – radio continuum: stars – X-rays: stars – stars: individual: GX 339−4

1. Introduction

Since its discovery in 1973 by the X-ray satellite *OSO-7* (Markert et al. 1973), the black hole candidate (BHC) GX 339−4 has been the subject of many extensive studies from the radio bands to the hard X-rays. Nevertheless, the physical processes involved in its broadband energy spectra have not been fully identified and understood. As the source has displayed a wide range of accretion rates – it is one of the rare sources that has been observed in all canonical black hole X-ray states – it is a prime target for studying the accretion-ejection processes of accreting black hole systems (persistent or transient). Among the canonical states, it is perhaps the low/hard state (LHS) that has attracted the most attention in recent years. Observations of various components in the LHS spectral energy distribution (SED) have highlighted analogies with the flat spectra of low-luminosity active galactic nuclei (AGN) (Falcke & Biermann 1996).

Radio emission from GX 339−4 during the LHS is characteristic of a self-absorbed compact jet (Corbel et al. 2000), similar to that considered for flat spectrum AGNs (Blandford & Königl 1979). Regular radio observations have shown that

the compact jet of GX 339−4 was quenched in the high/soft state (Fender et al. 1999; Corbel et al. 2000). Similar properties have now been observed in a growing number of persistent and transient BHCs (the jet has even been resolved in Cyg X−1, Stirling et al. 2001), thus suggesting that compact jets are ubiquitous in BHCs during the LHS (Fender 2001). In addition to being responsible for most of the emission in the radio regime, the compact jets may have a significant contribution in the infrared/optical bands (Corbel & Fender 2002) and could also be part of the processes involved in producing the X-ray emission (Markoff et al. 2001). In that case, it would imply that compact jets are very powerful and could dominate the entire SED of BHC during their low/hard states.

The other main components of the SED are a possible thermal contribution from the accretion disk, which extends from the near-infrared/optical to the soft X-rays, and the possible Comptonisation of accretion disk photons with a hot electron corona, which likely contribute mostly in soft and hard X-rays (Nowak et al. 2002; Done 2002). Despite not being observed, the companion star in the GX 339−4 system is likely an evolved low-mass star (Shahbaz et al. 2001; Chaty et al. 2002; Cowley et al. 2002).

A good way to assess the contribution of jets at high energy is to perform a broadband study of these systems

Send offprint requests to: S. Corbel,
e-mail: corbel@discovery.saclay.cea.fr

simultaneously at radio and X-ray frequencies, and in particular to study the correlation that could exist between these two emission domains. In fact, such a correlation has already been found for BHC in the LHS, e.g., GX 339−4 (Hannikainen et al. 1998; Corbel et al. 2000) and Cyg X−1 (Brocksopp et al. 1999) for BHC in the LHS. These radio/X-ray observations, however, only sampled a very limited range of X-ray and radio fluxes (or accretion rates). Most of these previous studies also suffered from the lack of sensitivity of the X-ray observations. A similar correlation also has been observed in the hard state of Cyg X−3 (McCollough et al. 1999; Choudhury et al. 2002). A more complex relation, but still indicating a relation between radio emitting electrons and the hard X-ray power law dominated state (like that in the LHS of BHC), is found in GRS 1915+105 (Klein-Wolt et al. 2002).

An interpretation for such a tight correlation is that it is the result of high energy synchrotron emission from the compact jet, as already has been proposed for XTE J1118+480 (Markoff et al. 2001). Alternatively, it possibly could be due to Compton scattering of photons from the companion star or the accretion flow off of the jet's leptons (Georganopoulos et al. 2002). In this paper, we report the results of a long-term study of GX 339−4 performed simultaneously in radio and X-ray during the years 1997–2000, in order to investigate the radio/X-ray correlation over many orders of magnitude with sensitive observations. Evidence for evolution of this correlation with energy is also presented. We discuss these results in light of the jet model of Markoff et al. (2003).

2. Observations

2.1. Radio observations

All radio observations were performed with the Australia Telescope Compact Array (ATCA). The ATCA synthesis telescope is an east-west array consisting of six 22 m antennas. The 8.6 GHz data that we used is from Corbel et al. (2000); however, we re-analysed all (five) observations for which the radio flux densities were weaker than 1 mJy. Further details concerning the ATCA and its data reduction can be found in Corbel et al. (2000). We also added the result of a series of three new ATCA observations, for a total duration of nearly 20 hours, performed on 2000 September 12, 15 and 18, during the recent off state. These observations provided a strong (99% confidence level) upper limit of 60 μJy at 8.6 GHz, which is the best constraint we have for the level of radio emission originating from GX 339−4 during its off state.

2.2. X-ray observations

2.2.1. RXTE

We used the *Rossi X-ray Timing Explorer* (*RXTE*) to perform a number of observations of GX 339−4 from 1997–1999, most of which represent the LHS. Analysis of the brightest of these observations was previously presented (Nowak et al. 2002); here we also consider analyses of faint, "off state" observations from late 1999. All data extractions were performed in an identical manner as that described by Nowak et al. (2002). The flux in various energy bands was determined by fitting a model comprised of neutral hydrogen absorption (N_{H} was fixed to 6×10^{21} cm^{-2}), a multi-temperature disk blackbody (e.g., Mitsuda et al. 1984) with peak temperature fixed at 0.25 keV, an exponentially cut-off broken power law with break energy at ≈ 10 keV, and a (potentially) broad Gaussian line with peak energy fixed at 6.4 keV. The faintest observations were fit with a simpler absorbed, single power law, plus (fixed peak energy) line feature. Feng et al. (2001) found that the iron line is shifted to higher energies when GX 339−4 was observed at low X-ray fluxes. However, this shift is not intrinsic to GX 339−4, but is rather due to the Galactic diffuse emission (Wardzinski et al. 2003). Note that due to differences between the two sets of instruments that comprise *RXTE*, the *Proportional Counter Array* (*PCA*, ≈ 3–20 keV) and the *High Energy X-ray Timing Experiment* (*HEXTE*, ≈ 20–200 keV), a normalization constant between the *PCA* and *HEXTE* detectors was used, and all flux values are normalized to the *PCA* flux levels (for further descriptions of this process, see Wilms et al. 1999). The flux error bars were chosen to be the larger of the statistical error, or 1%, which is a reasonable estimate of the RXTE internal systematic error (e.g., Wilms et al. 1999). Short timescale ($\lesssim$few seconds) X-ray variability is usually observed in the low-hard state of GX 339−4 (Smith & Liang 1999; Nowak et al. 2002). However, on a longer timescale (e.g. 10 min) the radio emission is steady (see Fig. 3 in Corbel et al. 2000) and so also is the X-ray spectrum of GX 339−4 integrated on those timescales (i.e., there is almost no very low frequency power in the power spectral densities, Nowak et al. 2002 and references therein). Therefore the error bars used in Table 1 are likely not affected by the variability of the source (which is quite steady on timescales greater than 10 min). Note that in Table 1 we quote the *absorbed* flux level; however, as we only consider energies ≥ 3 keV, this is at most a few percent different to the unabsorbed flux level.

RXTE has a broad $\approx 1°$ radius field of view, and therefore is potentially subject to contamination from faint background sources (or, in the case of GX 339−4, diffuse emission from the galactic ridge, Wardzinski et al. 2003). Four of the *RXTE* observations, however, were performed simultaneously with the much narrower field of view (≈ 4 arcmin radius) *Advanced Satellite for Cosmology and Astrophysics* (*ASCA*). Utilizing the same models described above, the 3–9 keV flux of the brightest two simultaneous observations determined by *ASCA* was 75–81% of that determined by the *PCA* – consistent with a well-known calibration offset between *PCA* and *ASCA* (see the discussion in Nowak et al. 2002). For the faintest two observations, the relative normalizations of the *ASCA* spectra substantially decreased with decreasing flux. This was taken as evidence for a faint background source or sources that lie within the field of view of the *PCA*, but not within the field of view of *ASCA*. The *RXTE* observation of 1999 July 29 is assumed to be heavily dominated by this contaminating source, and this spectrum, multiplied by 0.78, is subtracted as a "background correction" before model fitting and flux determination, from all *RXTE* observations occurring later than the observation of May 14 1999. With this additional background subtracted,

Table 1. Observing log of the simultaneous X-ray (PCA, unless otherwise noted) and radio (8.6 GHz) observations of GX 339−4 performed during a low/hard state. X-ray absorbed fluxes are all normalized to PCA. Upper limits are given at the one sigma level.

Date	X-ray flux				Radio flux density
	3–9 keV	9–20 keV	20–100 keV	100–200 keV	8.6 GHz
(y.m.d.)	$(10^{-10}$ erg s^{-1} cm^{-2})				(mJy)
1997.02.03	10.74 ± 0.11	10.28 ± 0.10	29.05 ± 0.29	11.57 ± 0.12	9.10 ± 0.10
1997.02.10	9.41 ± 0.09	9.10 ± 0.09	26.81 ± 0.27	10.74 ± 0.11	8.20 ± 0.10
1997.02.17	9.02 ± 0.09	8.73 ± 0.09	25.50 ± 0.26	10.49 ± 0.11	8.70 ± 0.10
1999.02.12	4.76 ± 0.05	4.21 ± 0.04	11.80 ± 0.12	4.16 ± 0.40	4.60 ± 0.08
1999.03.03	4.75 ± 0.05	4.62 ± 0.05	14.91 ± 0.15	6.66 ± 0.32	5.74 ± 0.06
1999.04.02	4.93 ± 0.05	4.90 ± 0.05	15.87 ± 0.16	8.75 ± 0.45	5.10 ± 0.07
1999.04.22	2.30 ± 0.02	2.34 ± 0.02	7.37 ± 0.10	4.04 ± 0.36	3.11 ± 0.04
1999.05.14	0.76 ± 0.01	0.74 ± 0.01	2.23 ± 0.17	1.39 ± 0.29	1.44 ± 0.04
1999.06.25	0.059 ± 0.006	0.052 ± 0.005	<0.17	<0.29	0.24 ± 0.05
1999.07.07	0.029 ± 0.002	<0.01	<0.17	<0.33	0.12 ± 0.04
1999.07.29	<0.008	<0.012	<0.16	<0.29	<0.036
1999.08.17[a]	0.025 ± 0.003	0.019 ± 0.014	0.110 ± 0.046	<0.05	0.27 ± 0.07
1999.09.01[b]	0.037 ± 0.003	<0.01	<0.17	<0.29	0.32 ± 0.05
2000.09.10[c,d]	0.0057 ± 0.001	<0.0034	<0.005	<0.07	<0.02

[a] Flux (or upper limits) above 9 keV are deduced from the BeppoSAX observations performed on 1999.08.13.

[b] Average X-ray flux, based on the PCA observations on 1999.08.28 and 1999.09.04.

[c] Radio observations on 2000.09.12, 2000.09.15 and 2000.09.18.

[d] X-ray observations performed by BeppoSAX.

the *ASCA* determined fluxes of the faintest two simultaneous observations become 73% and 83% of the corrected *PCA* 3–9 keV flux levels. Good agreement also is obtained between the *ASCA* and the corrected *PCA* spectra.

2.2.2. BeppoSAX

During the recent off state of GX 339−4 we conducted an ∼50 ks X-ray observation with *BeppoSAX* on September 10 2000. GX 339−4 is detected in the 1–10 keV energy range with both LECS and MECS, and the spectrum can be fitted with a power-law with a photon index 2.22 ± 0.24 (90% confidence level) with interstellar absorption fixed to 5.1×10^{21} cm^{-2} ($\chi_0^2 = 0.74$ for 35 degrees of freedom). The absorbed flux in the 3–9 keV energy range is 5.7×10^{-13} erg cm^{-2} s^{-1} (relative to the MECS normalization). To within a few percent, the fluxes normalized to MECS are consistent with the ones normalized to PCA (e.g. Della Ceca et al. 2001). We also re-analysed the BeppoSAX observation performed on August 13 1999 by Kong et al. (2000), as it was close to the date of one of our radio observations. All measurements (radio and X-ray) are tabulated in Table 1.

3. An extremely strong correlation between radio and X-ray emissions during the low/hard state

In Figs. 1 to 4, we utilize the results from Table 1 and display the radio flux density at 8.6 GHz versus the X-ray flux in different energy bands. It is apparent from these plots that a strong correlation exists between these two emission regimes in GX 339−4. As all these measurements have been taken during the low/hard state or during the transition to the off state (which appears to be a weak luminosity version of the low/hard state), we can further deduce that this correlation is a property of the low/hard state. We note that this strong correlation extends over more than three orders of magnitude in X-ray flux (e.g. the 3–9 keV band for which we have the best coverage). The correlation appears to hold for the entire four year period covered by the observations. Specifically, the 1997 measurements lie on the same line as the measurements performed during the transition to the off state in 1999 (Figs. 1 to 4), even though there was a transition to the soft state between these sets of observations (Belloni et al. 1999; Nowak et al. 2002).

In order to quantify the level of the correlation, we have calculated for each of the X-ray bands the Spearman rank correlation coefficient (Barlow 1989) between the radio and X-ray fluxes (Table 2). For this calculation, all detections have been taken into account (i.e. including even the points which are not strictly simultaneous or affected by a small reflare in hard X-rays: 1999.08.17 and 1999.09.01). It is clear from this analysis that the relationship between the radio and the soft and hard X-ray fluxes is extremely strong (a Student's t-test (Barlow 1989) shows the significance of the correlation is greater than 99.9% for each of the energy bands). This points to a persistent coupling between the mechanism(s) of the origin of the
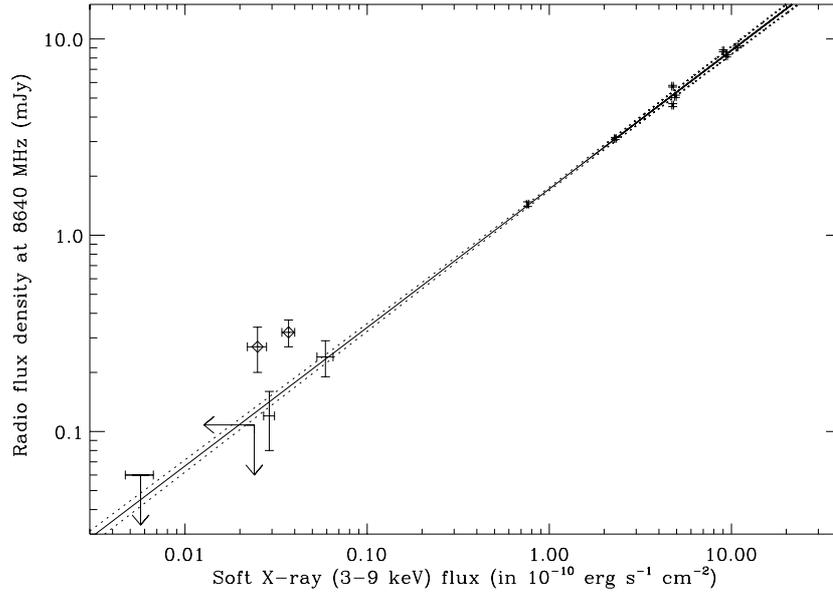
Fig. 1. The radio flux density at 8.6 GHz is plotted versus the X-ray flux in the 3–9 keV energy band. The continuous line denotes the fit to the data with the function described in the body of the paper and with the parameters estimated in Table 3, the dotted line represents the one-sigma deviation to those parameters. Upper limits are plotted at the three sigma level. The diamond points are those points that are not strictly simultaneous (1999.08.17) or maybe affected by a small reflare observed in hard X-rays (1999.09.01, see Fig. 15 in Corbel et al. 2000).
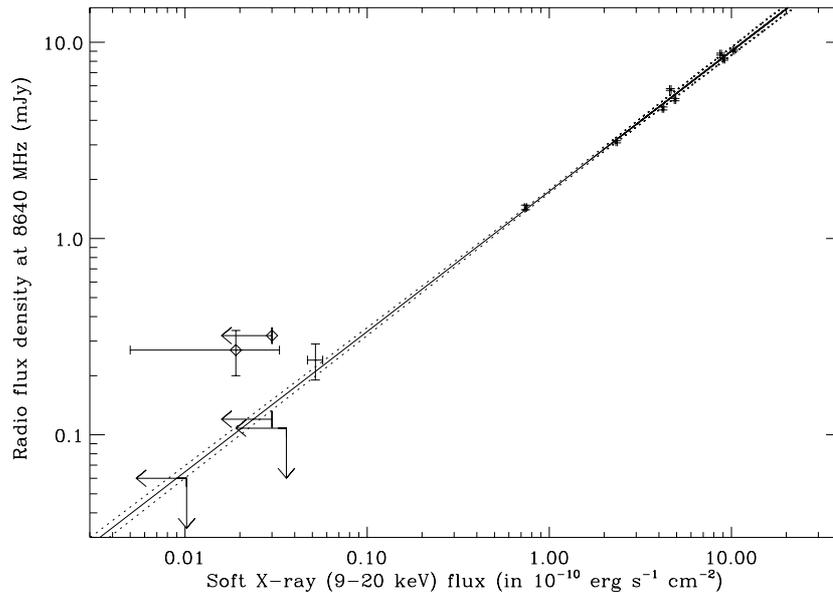

Fig. 2. Same as Fig. 1, but for the X-ray flux in the 9–20 keV energy band.

radio and X-ray emissions while GX 339−4 is in the low/hard state. This is the strongest evidence to date for such a persistent relation.

It is possible to estimate a functional relationship between the flux densities in radio (e.g. 8.6 GHz) and in the various X-ray bands. A linear fit (on a log-log scale) is satisfactory for the four X-ray bands. If we denote $F_{\rm Rad}$ as the radio flux density (in mJy) at 8.64 GHz and $F_{\rm X}$ as the X-ray flux (in units of $10^{-10}\,{\rm erg\,s^{-1}\,cm^{-2}}$) in a given energy band, the relation between these two fluxes can be expressed as $F_{\rm Rad} = a \times F_{\rm X}^{b}$, where a and b are the two constant coefficients given in Table 3. These relations are valid while GX 339−4 is in the standard

low/hard state, as we recall that radio emission from GX 339−4 is quenched in the high/soft state (Fender et al. 1999; Corbel et al. 2000).

As the same correlation appears to be maintained over this four year period, it could be realistic to estimate the level of radio emission from GX 339−4 by only measuring its X-ray flux. We note that little scatter is observed around the fitting function for our measurements. This also indicates that there is probably little time delay between the radio and X-ray emission. We also note the index b apparently changes with X-ray energy band. This is consistent with previous X-ray observations that indicate that, with the hard state, the spectrum of GX 339−4
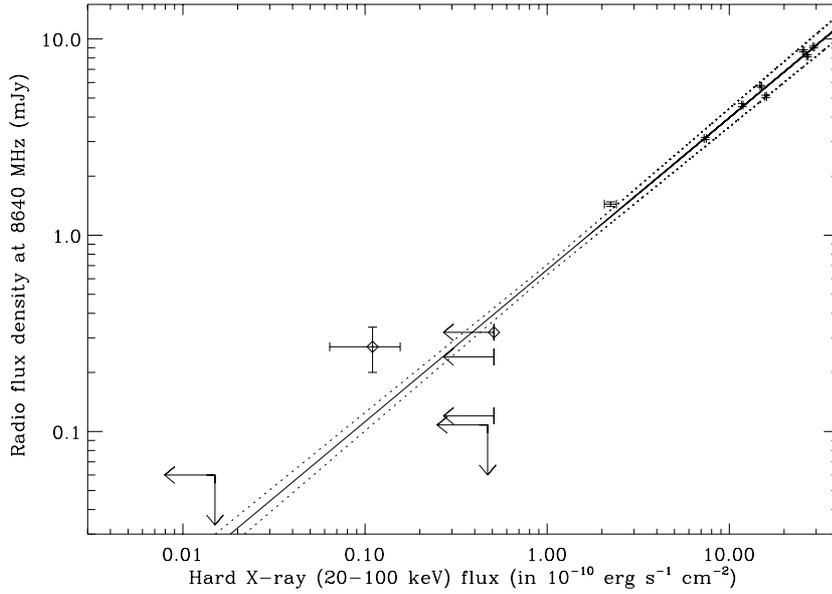
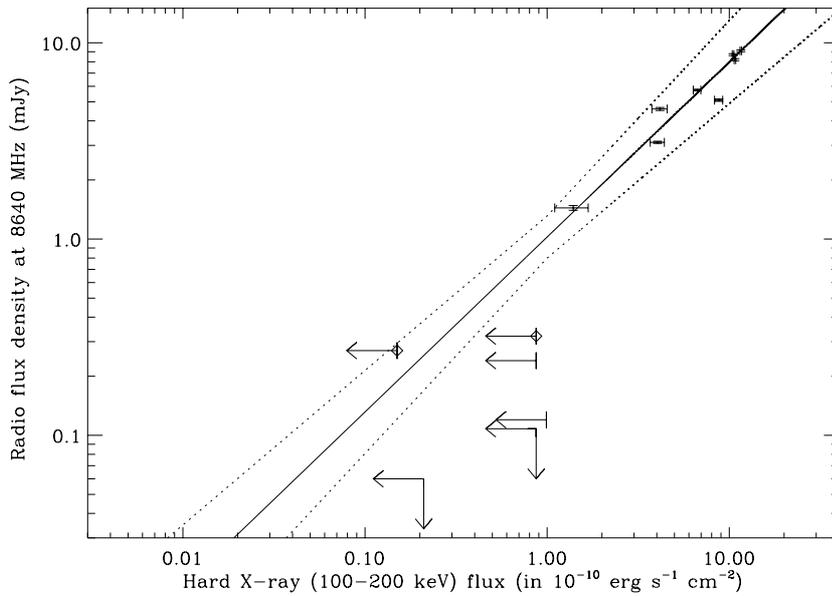**Fig. 3.** Same as Fig. 11, but for the X-ray flux in the 20–100 keV energy band.

Fig. 4. Same as Fig. 1, but for the X-ray flux in the 100–200 keV energy band.

Table 2. Spearman rank correlation coefficient, r_s, and the two sided significance of its deviation from zero, p, between the radio flux density measured at 8.6 GHz and the X-ray flux measured in various energy bands. The number of data-points, N, used in the calculations is also indicated in the last column.

X-ray band	r_s	p	N
3–9 keV	0.94	7.0×10^{-7}	12
9–20 keV	0.96	7.3×10^{-6}	10
20–100 keV	0.97	2.2×10^{-5}	9
100–200 keV	0.95	2.6×10^{-4}	8

becomes spectrally harder as the source becomes fainter (e.g., Nowak et al. 2002).

4. Discussions

With this study, we showed that the previously observed correlation between X-ray and radio fluxes during the low-hard state of GX 339−4 (Hannikainen et al. 1998; Corbel et al. 2000) extends over more than three decades in X-ray luminosity. The observations, spread over almost four years, indicated that the same fitting functions probably hold during these years, despite an intervening state transition. The radio emission in GX 339−4 is likely associated with the optically thick synchrotron emission from the compact jet (Corbel et al. 2000). The very strong correlation of radio emission with X-ray flux indicates that synchrotron processes may also play a role at high energies.

Table 3. Parameters of the function used to fit the radio flux density (in mJy) at 8.6 GHz, F_{Rad}, versus the flux, F_{X}, measured in a given energy band ((in unit of $10^{-10}\,\mathrm{erg\,s^{-1}\,cm^{-2}}$). The relation is expressed as $F_{\mathrm{rad}} = a \times F_{\mathrm{X}}^{b}$.

X-ray band	a	b
3–9 keV	1.721 ± 0.035	0.706 ± 0.011
9–20 keV	1.739 ± 0.035	0.715 ± 0.011
20–100 keV	0.667 ± 0.041	0.774 ± 0.021
100–200 keV	1.024 ± 0.287	0.891 ± 0.104

It has already been pointed out for GX 339−4 that the near infrared/optical bands show a spectral break that may indicate that the X-ray spectrum is an extension of the optically thin synchrotron emission from the compact jet (Corbel & Fender 2002). Specifically, the infrared points are consistent with an extrapolation of the slope from the radio, while the infrared/optical break extrapolates to the observed X-rays. The jet model, originally developed for AGN and previously applied to XTE J1118+480 (Markoff et al. 2001), has been further improved and also applied to these datasets (with additional optical data), and is discussed in a companion paper (Markoff et al. 2003). Markoff et al. (2003) showed that the jet model can account for the broadband spectra of GX 339−4 radio through optical through X-ray, primarily by only changing two parameters: the jet power and the location of the acceleration zone. The fact that the correlation holds at very low X-ray luminosity indicates that a compact jet is also produced when the source is close to quiescence. Therefore, the broadband emission of the jets has to be taken into account when studying the bolometric luminosity of black hole in quiescence, e.g. Campana & Stella (2000) and Garcia et al. (2001).

It is interesting to note that the radio flux at 8.6 GHz is proportional to the X-ray flux as $F_{\mathrm{rad}} \propto F_{\mathrm{X}}^{+0.71}$ (in the 3–9 and 9–20 keV bands) and that the same behaviour with the same index b has recently been found to hold for the black hole transient V404 Cyg (Gallo et al. 2002). The jet model of Markoff et al. (2003) successfully explains this dependency analytically using the formalism developed in Falcke & Biermann (1996). Indeed, if the only varying parameter of the model is the power in the jet, then the X-ray flux is expected to vary as $F_{\mathrm{X}} \propto F_{\mathrm{rad}}^{+1.41}$, i.e. $F_{\mathrm{rad}} \propto F_{\mathrm{X}}^{+0.71}$, completely consistent with the behaviour of GX 339−4 and V404 Cyg. The current versions of the jet model, however, do not account for the evolution of the exponent, b, in $F_{\mathrm{rad}} \propto F_{\mathrm{X}}^{b}$, for the higher energy X-ray bands, as is found for GX 339−4 (Table 3). If a jet is the underlying cause of the overall radio/X-ray correlation, the model may need to be further developed in order to explain this detailed behavior. However, it is important to point out that these higher energies include the canonical "100 keV cutoff" region in the data, where one expects the X-rays to decrease in comparison to the radio emission. However, the simplified accretion disk model used by Markoff et al. (2003) currently does not include all spectral components, e.g., the contribution from reflection which are often observed in the hard state X-ray spectra of BHC (e.g., Done 2002). Studies like these clearly show,

however, that including jet emission processes in any models of BHC spectra in their low/hard state is crucially important to fully understand the physical processes in these sources.

References

Barlow, R. J. 1989, in Statistics: A Guide to the Use of Statistical Methods in the Physical Sciences (John Wiley & Sons)
Blandford, R. D., & Königl, A. 1979, ApJ, 232, 34
Brocksopp, C., Fender, R. P., Larionov, V., et al. 1999, MNRAS, 309, 1063
Belloni, T., Méndez, M., van der Klis, M., Lewin, W. H. G., & Dieters, S. 1999, ApJ, 519, L159
Campana, S., & Stella, L. 2000, ApJ, 541, 849
Chaty, S., Mirabel, I. F., Goldoni, P., et al. 2002, MNRAS, 331, 1065
Choudhury, M., Rao, A. R., Vadawale, S. V., Ishwara-Chandra, C. H., & Jain, A. K. 2002, A&A, 383, L35
Corbel, S., Fender, R. P., Tzioumis, A. K., et al. 2000, A&A, 359, 251
Corbel, S., & Fender, R. P. 2002, ApJ, 573, L35
Cowley, A. P., Schmidtke, P. C., Hutchings, J. B., & Crampton, D. 2002, AJ, 123, 1741
Della Ceca, R., Pellegrini, S., Bassani, L., et al. 2001, A&A, 375, 781
Done, C. 2002, Philosophical Transactions of the Royal Society (Series A: Mathematical, Physical, and Engineering Sciences), submitted [astro-ph/0203246]
Falcke, H., & Biermann, P. L. 1996, A&A, 308, 321
Fender, R. P., Corbel, S., Tzioumis, A. K., et al. 1999, ApJ, 519, L165
Fender, R. P. 2001, MNRAS, 322, 31
Feng, Y. X., Zhang, S. N., Sun, X., et al. 2001, ApJ, 553, 394
Gallo, E., Fender, R. P., & Pooley, G. 2002, Proc. of the 4th Microquasar Workshop, ed. Ph. Durouchoux, Y. Fuchs, & J. Rodriguez [astro-ph/0207551]
Garcia, M. R., McClintock, J. E., Narayan, R., et al. 2001, ApJ, 553, L47
Georganopoulos, M., Aharonian, F. A., & Kirk, J. G. 2002, A&A, 388, L25
Hannikainen, D. C., Hunstead, R. W., Campbell-Wilson, D., & Sood, R. K. 1998, A&A, 337, 460
Klein-Wolt, M., Fender, R. P., Pooley, G. G., et al. 2002, MNRAS, 331, 745
Kong, A. K. H., Kuulkers, E., Charles, P. A., & Homer, L. 2000, MNRAS, 312, L49
Markert, T. H., Canizares, C. R., Clark, G. W., et al. 1973, ApJ, 184, L67
Markoff, S., Falcke, H., & Fender, R. 2001, A&A, 372, L25
Markoff, S., Nowak, M., Corbel, S., Fender, R., & Falcke, H. 2003, A&A, 397, 645
McCollough, M. L., Robinson, C. R., Zhang, S. N., et al. 1999, ApJ, 517, 951
Mitsuda, K., Inoue, H., Koyama, K., et al. 1984, PASJ, 36, 741
Nowak, M. A., Wilms, J., & Dove, J. B. 2002, MNRAS, 332, 856
Shahbaz, T., Fender, R., & Charles, P. A. 2001, A&A, 376, L17
Smith, I. A., & Liang, E. P. 1999, ApJ, 519, 771
Stirling, A. M., Spencer, R. E., de la Force, C. J., et al. 2001, MNRAS, 327, 1273
Wardzniski, G., Zdziarski, A. A., Gierlinski, M., et al. 2003, MNRAS, in press [astro-ph/0207598]
Wilms, J., Nowak, M. A., Dove, J. B., Fender, R. P., & di Matteo, T. 1999, ApJ, 522, 460